Am J Physiol Gastrointest Liver Physiol 294: G192–G198, 2008.
First published October 25, 2007; doi:10.1152/ajpgi.00122.2007.

Hepcidin inhibits apical iron uptake in intestinal cells

Natalia P. Mena, Andrés Esparza, Victoria Tapia, Pamela Valdés, and Marco T. Núñez

Departamento de Biología and Cell Dynamics and Biotechnology Research Center, Facultad de Ciencias, Universidad de Chile, Santiago, Chile

Submitted 9 March 2007; accepted in final form 23 October 2007

Mena NP, Esparza A, Tapia V, Valdés P, Núñez MT. Hepcidin inhibits apical iron uptake in intestinal cells. *Am J Physiol Gastrointest Liver Physiol* 294: G192–G198, 2008. First published October 25, 2007; doi:10.1152/ajpgi.00122.2007.—Hepcidin (Hepc) is considered a key mediator in iron trafficking. Although the mechanism of Hepc action in macrophages is fairly well established, much less is known about its action in intestinal cells, one of the main targets of Hepc. The current study investigated the effects of physiologically generated Hepc on iron transport in Caco-2 cell monolayers and rat duodenal segments compared with the effects on the J774 macrophage cell line. Addition of Hepc to Caco-2 cells or rat duodenal segments strongly inhibited apical ^{55}Fe uptake without apparent effects on the transfer of ^{55}Fe from the cells to the basolateral medium. Concurrently, the levels of divalent metal transporter 1 (DMT1) mRNA and protein in Caco-2 cells decreased while the mRNA and protein levels of the iron export transporter ferroportin did not change. Plasma membrane localization of ferroportin was studied by selective biotinylation of apical and basolateral membrane domains; Hepc induced rapid internalization of ferroportin in J774 cells but not in Caco-2 cells These results indicate that the effect of Hepc is cell dependent: in macrophages it inhibits iron export by inducing ferroportin degradation, whereas in enterocytes it inhibits apical iron uptake by inhibiting DMT1 transcription. Our results highlight the crucial role of Hepc in the control of intestinal iron absorption.

intestinal iron absorption; divalent metal transporter 1; ferroportin

DESPITE RECENT INTENSIVE RESEARCH efforts, the mechanisms that regulate intestinal iron absorption according to the content of iron stores are not fully understood. Hepc [also termed LEAP-1 (12)] has been proposed to act as a regulator of iron stores, a factor that signals the body iron content to intestinal cells, determining the amount of absorbed iron (19, 21). Hepc is produced in the liver as an 84-amino acid propeptide, which is cleaved to a 25-residue peptide before secretion into the blood (12). The mature peptide contains eight cysteine residues that form four disulfide bonds (20); this unusually high number of cysteine residues is common to antimicrobial peptides such as the defensins (23), tachyplesin (15), and protegrin (4).

Hepc has an important role in the control of body iron stores: mice with a disruption of the gene encoding the transcription factor Usf2 fail to produce Hepc mRNA and develop spontaneous iron overload in the liver and pancreas (19). Iron loading induces Hepc upregulation in mice (21), and mutations in the Hepc gene produce severe juvenile hemochromatosis (22).

The mechanisms by which Hepc regulates intestinal iron absorption are unclear. When Caco-2 cells, an intestinal epithelial cell line, are exposed to synthetic Hepc for 24 h, apical iron uptake is decreased, accompanied by a decrease in divalent metal transporter 1 (DMT1) protein and mRNA expression (25). Similarly, synthetic Hepc injected into mice has been shown to significantly inhibit the uptake phase of duodenal iron absorption without affecting the proportion of iron transferred to the circulation (14). In both reports, however, Hepc concentrations 10 to 100 times higher than those reported in serum or urine were used. In addition, synthetic Hepc may lack the precise disulfide bridging attained by the native peptide in the endoplasmic reticulum, and thus may represent a mixture of active and inactive forms. In contrast, it has been shown that stimulation of Hepc production by lipopolysaccharide injection induces a transient reduction of intestinal ferroportin mRNA at 6 h, followed by an increase at 48 h after injection (27). This increase in intestinal ferroportin mRNA contrasts with a model for Hepc activity developed in HEK-293 and HeLa cells, which demonstrated that Hepc promotes ferroportin internalization and degradation (18). Ferroportin downregulation in response to Hepc was also noted in bone marrow macrophages and J774 macrophage cells, in which Hepc decreased ferroportin protein levels and cell surface localization (5).

The results reported in macrophages and in HeLa and HEK-293 cells have been extrapolated to explain the effect of Hepc in the absorptive enterocyte (6, 18), although no direct experimental evidence has been provided. Indeed, the regulation of the different components of the iron homeostasis machinery may well be cell specific. A striking example of a cell-specific response is found in the regulation of ferroportin expression in enterocytes and alveolar macrophages. In enterocytes, ferroportin is induced by iron deficiency, whereas in alveolar macrophages, ferroportin is induced by iron supplementation (16, 26).

To discern the role of Hepc in iron absorption by intestinal cells, we designed the current study to investigate the action of native Hepc on cultured intestinal cells and duodenal segments compared with its effects on J774 macrophages. Our results show that in intestinal cells, Hepc decreased apical iron uptake and the expression of the iron transporter DMT1 but not that of ferroportin, in contrast with its action on J774 macrophages, where it transiently decreased ferroportin levels. These results provide evidence for cell-specific mechanisms in Hepc action and indicate that regulation of DMT1 expression is a crucial activity of Hepc in intestinal cells.

MATERIALS AND METHODS

Medium and reagents. The 25-residue COOH-terminal Hepc peptide (DTHFPICIFCCGCCHRSKCGMCCKT) was purchased

Address for reprint requests and other correspondence: Prof. M. T. Núñez, Departamento de Biología, Facultad de Ciencias, Universidad de Chile, Las Palmeras 3425, Santiago, Chile (e-mail: mnunez@uchile.cl).

The costs of publication of this article were defrayed in part by the payment of page charges. The article must therefore be hereby marked "*advertisement*" in accordance with 18 U.S.C. Section 1734 solely to indicate this fact.

from Bio-Synthesis (Lewisville, TX) and was subsequently used to generate an antibody against Hepc (see *Antibodies*). Cell culture media and reagents were purchased from Invitrogen (Carlsbad, CA). Cyanogen bromide (CNBr)-activated Sepharose, buffers, and other biochemical reagents were obtained from Sigma Chemical (St. Louis, MO).

Antibodies. The rabbit polyclonal antibodies anti-DMT1, prepared against the COOH-terminal end of the iron-responsive element (IRE)-containing DMT1 isoform, and anti-ferroportin, raised against the consensus sequence of human, rat, and mouse ferroportin, were made and utilized as described previously (19). Anti-Hepc was prepared by Biosonda (Santiago, Chile) via rabbit immunization with the refolded 25-residue synthetic COOH-terminal Hepc peptide following a published procedure (13). Before use, anti-Hepc was purified by affinity chromatography using the Hepc peptide bound to CNBr-activated Sepharose according to the manufacturer's instructions. The resulting antibody recognized a band of 10 kDa in cell extracts from HepG2 cells (vide infra). The secondary antibodies Alexa Fluor 488 goat anti-rabbit IgG and Alexa Fluor 594 goat anti-mouse IgG were purchased from Invitrogen and used according to the manufacturer's instructions.

Cell cultures and iron challenge. HepG2 hepatoma cells (ATCC CCL-131), Caco-2 human intestinal epithelial cells (ATCC HTB-37), and J774 rat macrophage cells (ATCC TIB-67) were grown at 37°C with 5% CO_2 in Dulbecco's modified Eagle's medium (DMEM) supplemented with 10% heat-inactivated fetal bovine serum, 15 mM HEPES, 10 mM nonessential amino acids, 0.5 mM sodium pyruvate (HepG2 cells only), 5.9 mM sodium bicarbonate, 10 U/ml penicillin, 10 mg/ml streptomycin, and 250 μg/ml fungizone. The culture medium was changed every 2 days. For ^{55}Fe uptake experiments, Caco-2 cells grown in Transwell inserts were challenged from the apical side with DMEM containing 5 μM $^{55}FeCl_3$-sodium nitrilotriacetate (NTA) (1:2.2 mol/mol) as described previously (24). After incubation, cell-associated ^{55}Fe and the ^{55}Fe content of the basolateral chamber were quantified. Total cell ^{55}Fe uptake (^{55}Fe in the cells plus basolateral medium) and transepithelial transport (^{55}Fe content in the basolateral medium) were determined and expressed as picomoles of ^{55}Fe per milligram of total cell protein. All measurements were performed in triplicate.

Cloning of a full-length Hepc cDNA. Total RNA was extracted from HepG2 cells using TRIzol reagent (Invitrogen) according to the manufacturer's instructions. To obtain a full-length human Hepc cDNA (GenBank accession no. AF309489), we performed reverse transcription-polymerase chain reaction (RT-PCR) amplification using the following primers: 5′-CAGACAGAATTCACGATGG-CAATGAGC-3′ (forward) and 5′-CAGGTAGCTCGAGCGTCTT-GCAGC-3′ (reverse). After initial denaturation at 94°C for 3 min, reactions were subjected to 30 cycles of 94°C for 30 s, 61°C for 1 min, and 72°C for 30 s, followed by a final 5-min elongation step at 72°C. Amplification products were observed on 1% agarose gels stained with ethidium bromide. The cDNA obtained was purified using a silica matrix in a solution of 6 M NaI and cloned into the pCDNA3 plasmid (Invitrogen). Inactive Hepc was obtained by the serendipitous insertion of a guanine at position 194 of the Hepc open reading frame during cloning. The insertion changed the reading frame at amino acid 65, resulting in a Hepc with an unrelated COOH-terminal domain that was shown to be inactive (see RESULTS). The construct was cloned into pCDNA3 and named pCDNA3-iHepc.

Cell transfections and preparation of Hepc-conditioned medium. Human hepatoma HepG2 cells grown in 60-mm wells were transiently transfected with a mix of 8 μg pCDNA3 containing the Hepc cDNA and 20 μl of Lipofectamine 2000 in 1 ml of Opti-MEM medium (Invitrogen-GIBCO Life Technologies). The cells were transfected for a second time after 24 h under the same conditions. Six hours after the second transfection, the Opti-MEM medium was supplemented with 40 μM iron, and incubation continued for another 48 h. The conditioned medium was then treated with Chelex resin to eliminate excess iron, filtered through a 10-kDa molecular weight cutoff Centricon centrifugal filter unit (Millipore, Billerica, MA), brought up to 3 μM iron (the content of iron in Opti-MEM) with Fe-NTA (1:2.2 mol/mol), and stored at −20°C. Control medium was obtained in a similar way from cells transfected with the empty pCDNA3 plasmid.

Antibody-depleted Hepc-conditioned medium. Hepc-depleted medium was prepared by treating Hepc-conditioned medium (prepared as above) with Sepharose-bound anti-Hepc overnight. To that end, anti-Hepc was affinity purified by absorption against the immunogenic peptide bound to Sepharose beads. The antibody was eluted with 0.2 M glycine, pH 2.5. After pH neutralization and dialysis against 0.5 M $NaHCO_3$, the purified antibody was coupled to CNBr-activated Sepharose beads. Control experiments determined the optimal ratio of antibody to medium. After separation of the Sepharose beads by centrifugation, the Hepc-depleted medium was stored at −20°C.

RT-PCR analysis. Total RNA was isolated from Caco-2 cells using TRIzol reagent. The PCR primers used to synthesize cDNA were as follows: DMT1 +IRE isoforms (GenBank accession nos. AF064481 and AF064482), 5′-CAGCCACTCAGGTACCCACCATGG-3′ (forward) and 5′-CTAATCCAGGGCCCTTTAACGTAGCCACGGG-3′ (reverse); ferroportin (GenBank accession no. AC012488), 5′-CCT-CCCAAACCGCTTCCAT-3′ (forward) and 5′-AAAAACAGAG-CAAAACACCCAGC-3′ (reverse); and β-actin (GenBank accession no. M10277), 5′-CCACACCCGCCGCCAGCTC-3′ (forward) and 5′-ATAGCACAGCCTGGATAGCAACGTACA-3′ (reverse). PCR was performed within the linear range of amplification with the following cycling parameters: DMT1, 36 cycles of 30 s at 94°C, 1

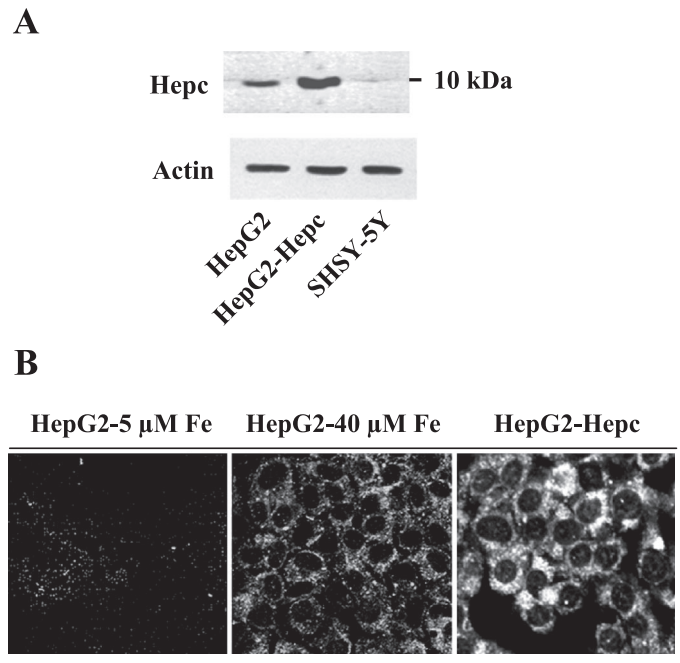

Fig. 1. Production of hepcidin (Hepc) by HepG2 cells. *A*: Western blot analysis of Hepc. Cell extracts from HepG2 cells transfected with Hepc (HepG2-Hepc) showed a readily detectable 10-kDa band, whereas nontransfected HepG2 cells showed a fainter band and the unrelated cell line SHSY-5Y showed undetectable levels of Hepc. Actin detection was included to control for load variations. *B*: immunofluorescence analysis of Hepc. HepG2 cells were transfected with the pcDNA3-Hepc plasmid (HepG2-Hepc) and incubated for 48 h as described in MATERIALS AND METHODS. Parallel cultures containing nontransfected HepG2 cells incubated with either 5 or 40 μM Fe (HepG2–5 μM Fe and HepG2–40 μM Fe, respectively) were also prepared. Cells were fixed, and Hepc was immunostained as described in MATERIALS AND METHODS. Images were obtained with a Zeiss 510 laser scanning confocal microscope. Representative frames of middle confocal sections are shown in the apical-basolateral axis.

min at 46°C, and 3 min at 72°C; ferroportin, 30 cycles of 1 min at 95°C, 90 s at 53°C, and 4 min at 68°C; and actin, 25 cycles of 30 s at 95°C, 1 min at 55°C, and 3 min at 75°C. Band intensities were quantified by densitometry and normalized by comparison with β-actin expression.

^{55}Fe uptake by rat duodenum. Fasting Fischer male rats from the Faculty of Medicine, University of Chile Animal Facility, were anesthetized by intraperitoneal injection of 30 mg/kg ketamine, and the duodenal section of the small intestine was isolated and flushed with ~5 ml of phosphate-buffered saline (pH 7.0) prewarmed to 37°C. Ligatures were made at the proximal and distal ends. The luminal side was filled with DMEM, and the duodenum was placed in a petri dish containing Hepc-conditioned culture medium and bathed for 6 h at 37°C under 5% CO_2. After this initial incubation, 5 μM ^{55}Fe-NTA was added to the intestinal lumen medium and the incubation continued for 2 h. ^{55}Fe uptake was stopped by washing the intestinal lumen six times with 2-ml aliquots of ice-cold phosphate-buffered saline supplemented with 1 mM EDTA. The amount of ^{55}Fe was then determined in homogenates of the duodenal tissue and in the bathing medium. The summation of both determinations was considered the total ^{55}Fe uptake by a duodenal segment. Uptake data was expressed as the percentage of uptake under the control (no Hepc) condition.

Biotinylation and Western blot analysis. The plasma membrane localization of ferroportin was studied by selective biotinylation as described previously (3). Briefly, cells were incubated for 30 min at 4°C with 0.5 mg/ml NHS-imino biotin (Pierce, Rockford, IL). After washing, cellular extracts were prepared (1) and incubated at 4°C overnight with 50% immobilized streptavidin (Pierce). The streptavidin-biotin pellet was dissolved in SDS loading buffer, boiled for 5 min, and resolved by 10% SDS-polyacrylamide gel electrophoresis. The proteins were then transferred to a nitrocellulose membrane for Western blot analysis. Western blot analysis of DMT1 and ferroportin was carried out as described previously (1). To detect Hepc, 100 μg of cell extract were resolved by electrophoresis on a 20% SDS polyacrylamide gel and transferred onto a nitrocellulose membrane. The membrane was incubated for 3 h in blocking solution (10 mM Tris·HCl, pH 8.0, 150 mM NaCl, 5% skim milk, and 0.05% Tween 20) followed by an overnight incubation with a 1:500 dilution of anti-Hepc. After washing in Tris-buffered saline, membranes were incubated with horseradish peroxidase-conjugated anti-rabbit IgG for 1 h at 25°C, and the immunoreactive band was detected with the peroxidase-based SuperSignal chemiluminescence assay kit (Pierce).

Immunocytochemistry. Caco-2 cells were cultured on glass slides with Hepc-conditioned culture medium for 48 h. The cells were fixed for 10 min with 4% paraformaldehyde and 4% sucrose and permeabilized with 0.2% Triton X-100 in phosphate-buffered saline. Overnight incubation with an antibody against Hepc, DMT1, or ferroportin was followed by incubation with Alexa Fluor 488 goat anti-rabbit IgG or Alexa Fluor 594 goat anti-mouse IgG, for 2 h. Immunostaining was observed using a Zeiss LSM 510 Meta confocal laser scanning microscope (Carl Zeiss, Göttingen, Germany).

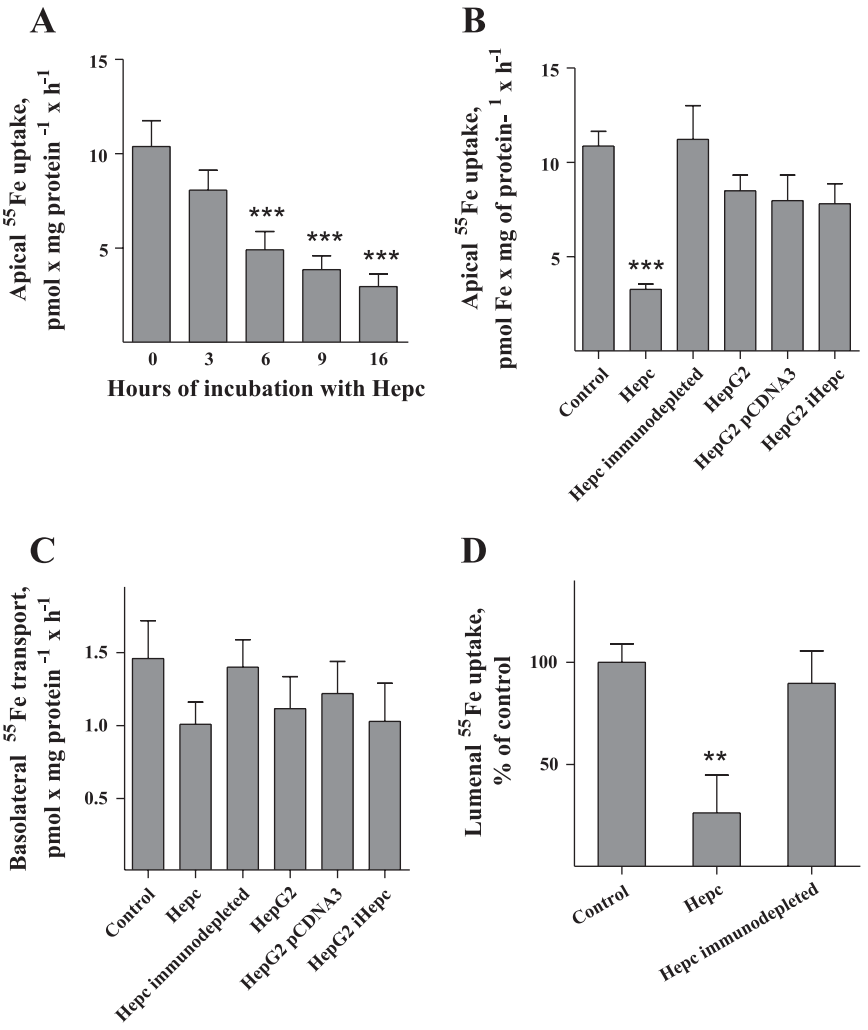

Fig. 2. Hepc inhibits ^{55}Fe uptake in rat duodenal segments and Caco-2 cells. *A*: effect of Hepc treatment on ^{55}Fe uptake by Caco-2 cells. Caco-2 cells grown in bicameral inserts were pretreated for the indicated times with Hepc-conditioned medium and then subjected to ^{55}Fe apical uptake for 1 h at 37°C as described in MATERIALS AND METHODS. Data are means ± SD from triplicate samples of 1 of 3 independent experiments. ***$P < 0.001$ compared with *time 0*. *B*: ^{55}Fe uptake by Caco-2 cells. Caco-2 cells grown in bicameral inserts were treated for 16 h with Opti-MEM culture medium without pretreatment (control) or pretreated with culture medium from nontransfected HepG2 cells (HepG2), culture medium from HepG2 cells transfected with the pCDNA3 plasmid (HepG2-pCDNA3), culture medium from HepG2 cells transfected with pCDNA3-Hepc (HepG2-Hepc), and culture medium from HepG2 cells transfected with the inactive Hepc mutant (HepG2-iHepc). The inserts were then challenged with ^{55}Fe from the apical side for 1 h at 37°C. ***$P < 0.001$ compared with control medium. *C*: transepithelial ^{55}Fe transport by Caco-2 cells. Caco-2 cells grown in bicameral inserts were treated with control, HepG2, HepG2-pCDNA3, HepG2-Hepc, and HepG2-iHepc medium as described in MATERIALS AND METHODS, and the ^{55}Fe contents of the basolateral chamber were quantified. ***$P < 0.001$ compared with control medium. *D*: ^{55}Fe uptake by rat duodenal intestine. Isolated duodenal sections were preincubated for 6 h at 37°C in petri dishes containing control culture medium, Hepc-conditioned medium, or Hepc-conditioned medium depleted of Hepc by treatment with anti-Hepc antibody bound to Sepharose. After the initial incubation, 5 μM $^{55}FeCl_3$-sodium nitrilotriacetate was added to the intestinal lumen medium, and the incubation was continued for 2 h. ^{55}Fe radioactivity was then determined in the duodenal tissue and in the bathing medium. ^{55}Fe uptake is expressed as a percentage of control uptake. **$P < 0.01$ compared with both control and immunodepleted media.

Data analysis. One-way ANOVA was used to test differences in mean values, and Tukey's post hoc test was used for comparisons (InStat; GraphPad Software, San Diego, CA). Differences were considered significant if $P < 0.05$.

RESULTS

Production of Hepc by HepG2 hepatoma cells. Western blot assays of cell extracts from control and Hepc-transfected HepG2 cells identified a 10-kDa immunoreactive band that corresponded with those described in guinea pig and human liver as well as in HepG2 cells (13). In contrast, the Hepc band was absent in cell extracts derived from the unrelated neuroblastoma cell line SHSY-5Y (Fig. 1*A*). Hepc immunostaining of cells cultured in 5 μM Fe revealed a basal signal corresponding to Hepc production under a nonstimulated condition, which increased in cells cultured in 40 μM Fe and in cells transfected with pCDNA3-Hepc (Fig. 1*B*). These results indicate that the antibody recognizes Hepc both in Western blots and immunostaining assays and that the transfection strategy produced a marked increase in Hepc expression. Moreover, the cells increased Hepc synthesis in response to increased iron in the medium.

Hepc-conditioned medium decreases apical ^{55}Fe uptake in Caco-2 cells and duodenal segments. Increased iron stores induce a response that includes increased liver Hepc synthesis followed by secretion of Hepc into the bloodstream (5, 7, 21). It is thought that secreted Hepc exerts its action on mature duodenal cells by inducing ferroportin degradation (6, 18), although evidence that Hepc inhibits apical uptake is also available (14). To assess whether Hepc modifies the activity of the iron transporters, we took advantage of the Caco-2 cell system grown on bicameral inserts, which allows for the determination of apical uptake and transepithelial iron transport (2, 24). Incubation of Caco-2 cells with Hepc-conditioned medium inhibited in a time-dependent way apical iron uptake by Caco-2 cells (Fig. 2*A*). Apical uptake was inhibited by 50% after 6 h of incubation and by 70% after 16 h. The strong inhibitory activity of Hepc-conditioned medium was completely abolished when the medium was first immunodepleted of Hepc (Fig. 2*B*). A nonsignificant inhibition of apical uptake was observed when cells were incubated with conditioned media derived from HepG2 and HepG2-pCDNA3 cells or with conditioned medium from HepG2 cells transfected with an inactive form of Hepc (Fig. 2*B*). Testing of this last condition was necessary to differentiate the effects of Hepc from the effects of other compounds that may have been released from the cells used to prepare the Hepc-conditioned medium. Hepc treatment also diminished the amount of ^{55}Fe found in the basolateral chamber, but the decrease did not reach significance compared with the control ($P < 0.07$) (Fig. 2*C*). Indeed, the amount of ^{55}Fe transferred to the basolateral medium seemed to reflect the amount of ^{55}Fe incorporated during the apical uptake phase, because when corrected for total ^{55}Fe uptake (^{55}Fe in cells plus ^{55}Fe in basolateral medium), no inhibition was apparent (data not shown). We then tested whether Hepc modified the capacity of duodenum segments to carry out iron uptake and transport. Toward that end, duodenum segments were preincubated from the serosal side with untreated control medium, Hepc-conditioned medium, or Hepc-immunodepleted medium. Hepc-conditioned medium induced a significant decrease in luminal ^{55}Fe uptake by duodenal segments compared with control medium ($P < 0.01$), an effect that was prevented when the medium was previously immunodepleted of Hepc (Fig. 2*D*). These results indicate that Hepc strongly inhibits apical iron uptake by intestinal cells but does not affect iron permeation through the basolateral membrane.

Effect of Hepc on the membrane distribution of ferroportin in Caco-2 cells and J774 macrophages. To determine whether the inhibition of apical iron uptake exerted by Hepc was secondary to an initial downregulation of ferroportin that subsequently resulted in iron accumulation and DMT1 downregulation, we investigated the membrane distribution of ferroportin at early times after addition of Hepc to polarized

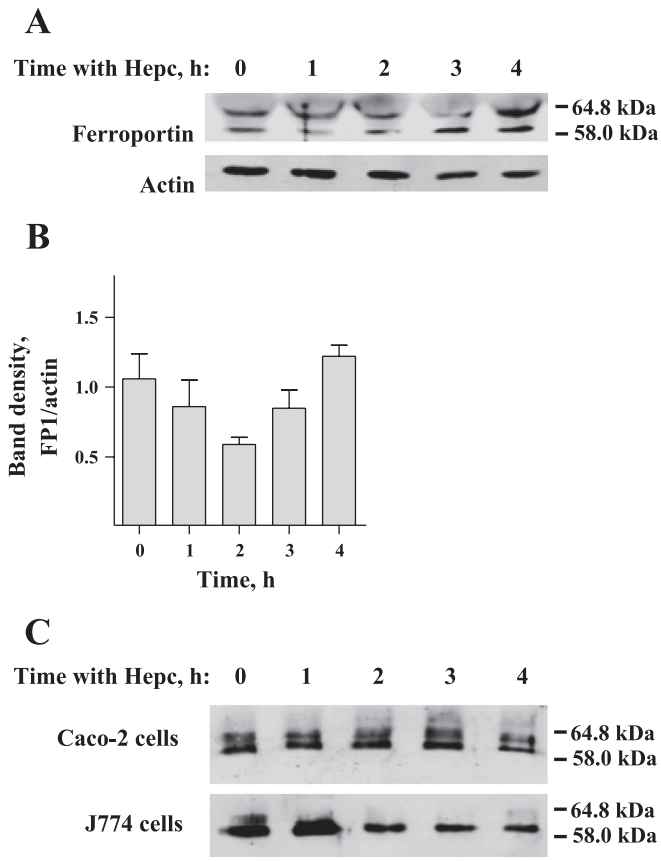

Fig. 3. Effect of Hepc on total and membrane-bound ferroportin (FP). *A*: total FP content in J774 cells. Cell extracts from J774 cells incubated with Hepc-enriched medium for the indicated times were analyzed for overall FP expression by Western blotting. Immunoreactive bands of 64.8 and 58 kDa were detected. Both bands were specific because they were not seen upon preincubation of the antiserum with the immunization peptide (data not shown). Actin immunodetection indicates protein loading between lanes. *B*: bands from *A* were quantified by densitometry and normalized for loading by β-actin (FP1/actin). Data represent means ± SD of 3 independent experiments. *C*: membrane biotinylation of FP. Caco-2 cells grown in bicameral inserts were incubated from the basolateral chamber with Hepc-enriched medium for the indicated times. Cells were then cooled to 4°C and biotinylated from the basolateral medium. Bands represent FP present in the basolateral membrane. As a positive control, the study was repeated in J774 cells, a macrophage cell line in which Hepc decreases FP content. Shown is 1 of 3 independent experiments of biotinylation.

Caco-2 cells. As a control, we observed the effect of Hepc treatment in the macrophage cell line J774, in which Hepc has been shown to decrease ferroportin protein levels (10, 11). We found that Hepc treatment decreased total (Figs. 3, *A* and *B*) and membrane (Fig. 3*C*) ferroportin content in J774 cells, as expected. In contrast, Hepc did not induce any significant decrease in membrane ferroportin in Caco-2 cells (Fig. 3*C*). The kinetics of total and membrane ferroportin localization in J774 cells differed, however. Total ferroportin content decreased after 1 h of Hepc treatment but increased to pretreatment levels by 3 h (Fig. 3, *A*and *B*), a behavior reminiscent of the Hepc-induced ferroportin fluctuations reported in rat intestine (27). Changes in membrane ferroportin were slower (Fig. 3*C*), decreasing after 2 h of Hepc treatment and remaining low for up to 4 h (Fig. 3*B*). These results corroborate previous data on the effect of Hepc in J774 cells (10) and show that the biotinylation methodology we used appropriately describes the membrane movements of ferroportin.

mRNA and protein expression of DMT1 and ferroportin. RNA from Caco-2 cells treated for 24 with Hepc-conditioned medium was analyzed for DMT1 and ferroportin mRNA expression by semiquantitative RT-PCR (Fig. 4*A*). DMT1 RT-PCR was performed on the DMT1(IRE) transcripts, because these splice variants are the isoforms that respond to variations in cell iron content (9). A twofold decrease in DMT1 mRNA expression was observed in Hepc-treated cells compared with cells treated with control medium (Fig. 4*B*). In contrast, changes in ferroportin mRNA expression were not readily apparent. To determine whether the decrease of DMT1 mRNA was due to a decreased rate of transcription or to an increased rate of degradation of the transcript, we analyzed transcript levels after treatment with the transcriptional inhibitor actinomycin D, in the absence or presence of Hepc (Fig. 4, *C*and *D*). There was no difference in the rate of degradation between control and Hepc-treated cells after a 6-h incubation. These results suggest that Hepc may regulate the expression of the DMT1 transporter and point to the differential effects of Hepc in intestinal and macrophage cells.

To investigate whether the changes in DMT1 and ferroportin mRNA expression translated into changes in protein content, we examined DMT1 and ferroportin levels in Caco-2 cells (Fig. 5*A*) or rat duodenal sections (Fig. 5*B*) by Western blotting. The DMT1 band decreased significantly in both Caco-2 cells and duodenal sections treated with Hepc-conditioned medium, whereas no changes were observed in ferroportin expression. These protein expression patterns are consistent with the iron uptake experiments reported in Fig. 3, where Hepc mostly affected ^{55}Fe uptake. They also agree with the RT-PCR results presented in Fig. 4, strongly suggesting that Hepc decreases expression of the iron import transporter DMT1 in Caco-2 cells.

DISCUSSION

The important role for Hepc in intestinal iron absorption was established in studies with Hepc knockout mice, which display severe tissue iron overload (19). Previous work demonstrated that Hepc reduces iron absorption in mice and

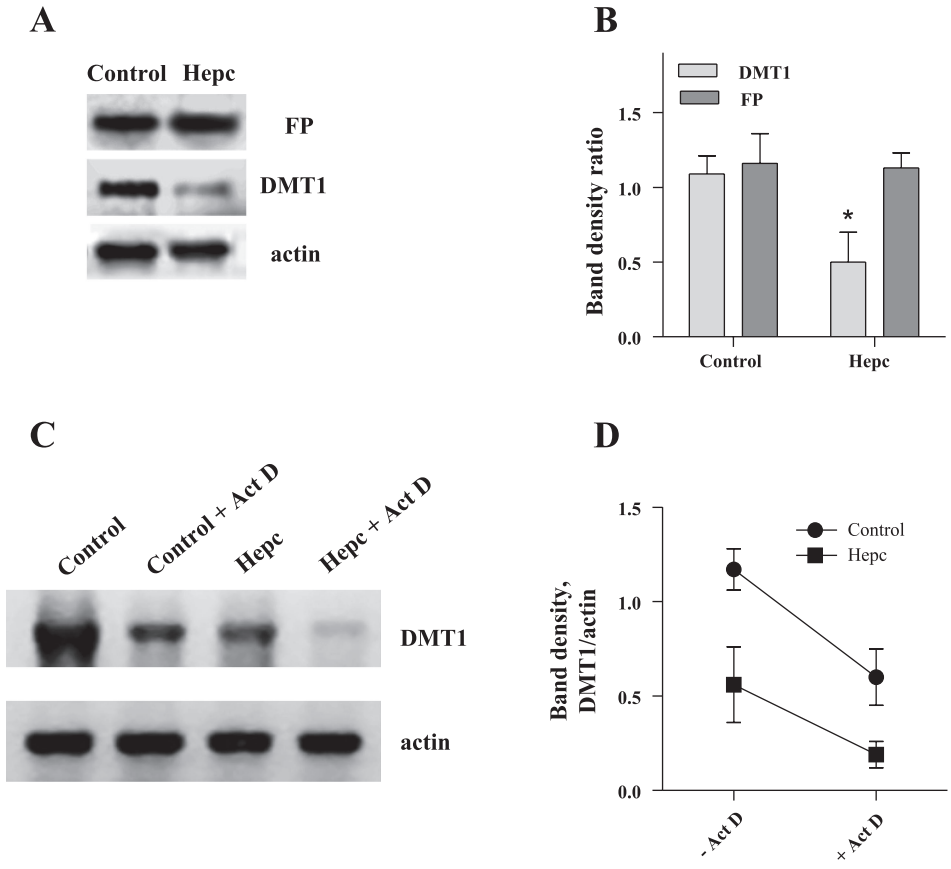

Fig. 4. Effect of Hepc on divalent metal transporter 1 (DMT1) and FP mRNA expression in Caco-2 cells. *A*: Caco-2 cells were incubated for 12 h in control or Hepc-conditioned medium. Total RNA was extracted, and DMT1 and FP gene expression was determined by semiquantitative RT-PCR. Actin mRNA expression was similarly analyzed as a loading control. *B*: band intensities from *A* were quantified by densitometry and normalized for loading by actin mRNA expression. Data represent means ± SD of 3 independent experiments. *P = 0.0119 compared with control cells. *C*: cells were incubated for 6 h in the presence or absence of 5 μg/ml of the transcriptional inhibitor actinomycin D (Act D). Total RNA was extracted, and DMT1 expression was determined by semiquantitative RT-PCR. Actin mRNA expression was similarly analyzed as a loading control. *D*: bands from *C* were quantified by densitometry and normalized for loading by β-actin mRNA expression. Data represent means ± SD of 3 independent experiments.

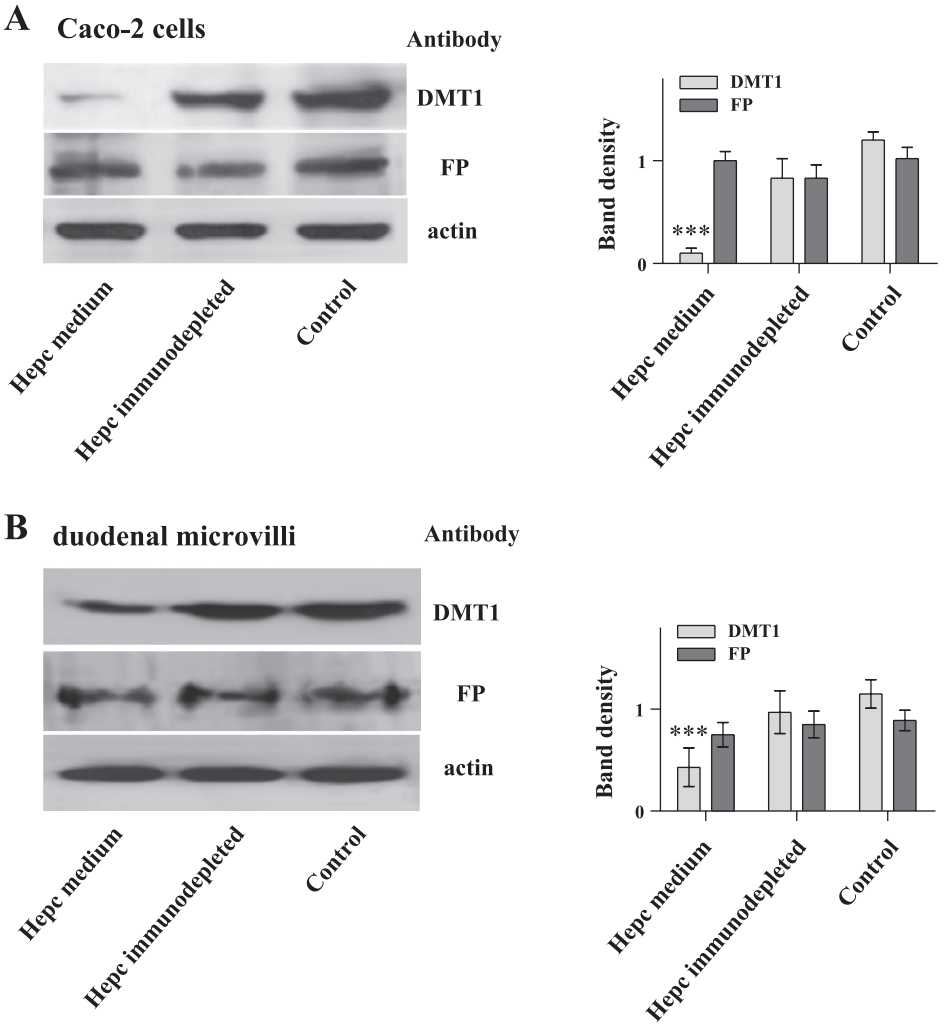

Fig. 5. Hepc inhibits DMT1 but not FP expression in Caco-2 cells and duodenal segments. *A*: Western blot analysis of DMT1 and FP from Caco-2 cells treated for 8 h with Hepc-conditioned medium (Hepc medium), Hepc-conditioned medium depleted of Hepc by treatment with anti-Hepc bound to Sepharose (Hepc-immunodepleted medium), or Opti-MEM medium without treatment (control). Western blot analysis of FP was done using stripped membranes previously used for DMT1 detection. Actin was immunoblotted as a loading control. Graph at *right* shows means ± SD ($n = 3$) of band densities from blot at *left*, normalized to β-actin. *B*: Western blot assay for DMT1 and FP from rat duodenal extracts. Duodenal segments were treated for 6 h with Hepc-conditioned medium (Hepc), Hepc-conditioned medium that was immunodepleted of Hepc, or Opti-MEM medium without treatment (control). Graph at *right* shows means ± SD of band densities ($n = 3$) from blot at *left*, normalized to β-actin. ***$P < 0.001$ compared with respective control.

Caco-2 cells (14, 25). However, the use of synthetic Hepc raised some uncertainty about the Hepc isomer responsible for the observed results. This uncertainty was compounded by ensuing reports indicating that Hepc promoted endocytosis and degradation of ectopically expressed ferroportin (5, 10, 11, 18) in non-intestinal cells (HEK-293, HeLa, and macrophages), which was subsequently extrapolated to suggest that Hepc regulates intestinal iron absorption through ferroportin internalization and degradation (6, 7). Yet, direct evidence of the mechanism by which Hepc regulates intestinal iron absorption has been either lacking or controversial.

Using Caco-2 cells and excised rat duodenum as model systems for absorptive epithelia, we found that Hepc concertedly decreased apical iron uptake, as well as DMT1 mRNA and protein expression, without affecting ferroportin expression. It follows that the decrease in apical iron uptake was most probably the consequence of a primary effect of Hepc on DMT1 gene transcription and not due to increased ferroportin degradation.

The observed Hepc-mediated DMT1 decrease agrees with a recent report in which decreased Hepc expression in rats correlated with increased duodenal DMT1 expression during iron deficiency and pregnancy (17). The same authors reported no changes in ferroportin mRNA and a mild increase in ferroportin protein levels, an indication of increased ferroportin stability under iron deficiency conditions. Similarly, decreased Hepc and increased duodenal DMT1 and ferroportin were reported in mice treated with 10–20% ethanol for 7 days (8). The DMT1 response was obliterated by antioxidants or injection of Hepc peptide, indicating that Hepc downregulates DMT1 expression whereas oxidative stress upregulates it. Collectively, these findings indicate that Hepc mediates a transcriptional response resulting in decreased duodenal DMT1 expression. Detailed knowledge of the pathways involved in this negative regulation requires further study.

The decrease in DMT1 expression in response to Hepc reported presently, combined with previously published evidence in J774 and HEK-293 cells, is consistent with a mechanism in which Hepc decreases circulating iron by decreasing luminal iron absorption in the intestine and by inhibiting iron exit from macrophages and renal epithelia. These findings point to cell-specific factors that mediate Hepc action. Identification and analysis of novel Hepc-responsive elements will open new avenues for examining the regulation of body iron levels.

ACKNOWLEDGMENTS

We are grateful to Dr. Cecilia Hidalgo for thoughtful comments on the manuscript.

GRANT

This work was financed by Fondo Nacional de Ciencia y Tecnología Grant 1070840.

REFERENCES

1. **Aguirre P, Mena N, Tapia V, Arredondo M, Núñez MT.** Iron homeostasis in neuronal cells: a role for IREG1. *BMC Neurosci* 6: 3, 2005.
2. **Alvarez-Hernandez X, Nichols GM, Glass J.** Caco-2 cell line: a system for studying intestinal iron transport across epithelial cell monolayers. *Biochim Biophys Acta* 1070: 205–208, 1991.
3. **Arredondo M, Tapia V, Rojas A, Aguirre P, Reyes F, Marzolo MP, Núñez MT.** Apical distribution of HFE-β2-microglobulin is associated with inhibition of apical iron uptake in intestinal epithelia cells. *Biometals* 19: 379–388, 2006.
4. **Aumelas A, Mangoni M, Roumestand C, Chiche L, Despaux E, Grassy G, Calas B, Chavanieu A.** Synthesis and solution structure of the antimicrobial peptide protegrin-1. *Eur J Biochem* 237: 575–583, 1996.
5. **Delaby C, Pilard N, Goncalves AS, Beaumont C, Canonne-Hergaux F.** Presence of the iron exporter ferroportin at the plasma membrane of macrophages is enhanced by iron loading and down-regulated by hepcidin. *Blood* 106: 3979–3984, 2005.
6. **Frazer DM, Anderson GJ.** Iron imports. I. Intestinal iron absorption and its regulation. *Am J Physiol Gastrointest Liver Physiol* 289: G631–G635, 2005.
7. **Ganz T.** Hepcidin—a peptide hormone at the interface of innate immunity and iron metabolism. *Curr Top Microbiol Immunol* 306: 183–198, 2006.
8. **Harrison-Findik DD, Schafer D, Klein E, Timchenko NA, Kulaksiz H, Clemens D, Fein E, Andriopoulos B, Pantopoulos K, Gollan J.** Alcohol metabolism-mediated oxidative stress down-regulates hepcidin transcription and leads to increased duodenal iron transporter expression. *J Biol Chem* 281: 22974–22982, 2006.
9. **Hubert N, Hentze MW.** Previously uncharacterized isoforms of divalent metal transporter (DMT)-1: implications for regulation and cellular function. *Proc Natl Acad Sci USA* 99: 12345–12350, 2002.
10. **Knutson MD, Oukka M, Koss LM, Aydemir F, Wessling-Resnick M.** Iron release from macrophages after erythrophagocytosis is up-regulated by ferroportin 1 overexpression and down-regulated by hepcidin. *Proc Natl Acad Sci USA* 102: 1324–1328, 2005.
11. **Knutson MD, Vafa MR, Haile DJ, Wessling-Resnick M.** Iron loading and erythrophagocytosis increase ferroportin 1 (FPN1) expression in J774 macrophages. *Blood* 102: 4191–4197, 2003.
12. **Krause A, Neitz S, Magert HJ, Schulz A, Forssmann WG, Schulz-Knappe P, Adermann K.** LEAP-1, a novel highly disulfide-bonded human peptide, exhibits antimicrobial activity. *FEBS Lett* 480: 147–150, 2000.
13. **Kulaksiz H, Gehrke SG, Janetzko A, Rost D, Bruckner T, Kallinowski B, Stremmel W.** Pro-hepcidin: expression and cell specific localisation in the liver and its regulation in hereditary haemochromatosis, chronic renal insufficiency, and renal anaemia. *Gut* 53: 735–743, 2004.
14. **Laftah AH, Ramesh B, Simpson RJ, Solanky N, Bahram S, Schumann K, Debnam ES, Srai SK.** Effect of hepcidin on intestinal iron absorption in mice. *Blood* 103: 3940–3944, 2004.
15. **Matsuzaki K, Nakayama M, Fukui M, Otaka A, Funakoshi S, Fujii N, Bessho K, Miyajima K.** Role of disulfide linkages in tachyplesin-lipid interactions. *Biochemistry* 32: 11704–11710, 1993.
16. **McKie AT, Marciani P, Rolfs A, Brennan K, Wehr K, Barrow D, Miret S, Bomford A, Peters TJ, Farzaneh F, Hediger MA, Hentze MW, Simpson RJ.** A novel duodenal iron-regulated transporter, IREG1, implicated in the basolateral transfer of iron to the circulation. *Mol Cell* 5: 299–309, 2000.
17. **Millard KN, Frazer DM, Wilkins SJ, Anderson GJ.** Changes in the expression of intestinal iron transport and hepatic regulatory molecules explain the enhanced iron absorption associated with pregnancy in the rat. *Gut* 53: 655–660, 2004.
18. **Nemeth E, Tuttle MS, Powelson J, Vaughn MB, Donovan A, Ward DM, Ganz T, Kaplan J.** Hepcidin regulates cellular iron efflux by binding to ferroportin and inducing its internalization. *Science* 306: 2090–2093, 2004.
19. **Nicolas G, Bennoun M, Devaux I, Beaumont C, Grandchamp B, Kahn A, Vaulont S.** Lack of hepcidin gene expression and severe tissue iron overload in upstream stimulatory factor 2 (USF2) knockout mice. *Proc Natl Acad Sci USA* 98: 8780–8785, 2001.
20. **Park CH, Valore EV, Waring AJ, Ganz T.** Hepcidin, a urinary antimicrobial peptide synthesized in the liver. *J Biol Chem* 276: 7806–7810, 2001.
21. **Pigeon C, Ilyin G, Courselaud B, Leroyer P, Turlin B, Brissot P, Loreal O.** A new mouse liver-specific gene, encoding a protein homologous to human antimicrobial peptide hepcidin, is overexpressed during iron overload. *J Biol Chem* 276: 7811–7819, 2001.
22. **Roetto A, Papanikolaou G, Politou M, Alberti F, Girelli D, Christakis J, Loukopoulos D, Camaschella C.** Mutant antimicrobial peptide hepcidin is associated with severe juvenile hemochromatosis. *Nat Genet* 33: 21–22, 2003.
23. **Schibli DJ, Hunter HN, Aseyev V, Starner TD, Wiencek JM, McCray PB Jr, Tack BF, Vogel HJ.** The solution structures of the human β-defensins lead to a better understanding of the potent bactericidal activity of HBD3 against *Staphylococcus aureus*. *J Biol Chem* 277: 8279–8289, 2002.
24. **Tapia V, Arredondo M, Núñez M.** Regulation of Fe absorption by cultured intestinal epithelia (Caco-2) cell monolayers with varied Fe status. *Am J Physiol Gastrointest Liver Physiol* 271: G443–G447, 1996.
25. **Yamaji S, Sharp P, Ramesh B, Srai SK.** Inhibition of iron transport across human intestinal epithelial cells by hepcidin. *Blood* 104: 2178–2180, 2004.
26. **Yang F, Wang X, Haile DJ, Piantadosi CA, Ghio AJ.** Iron increases expression of iron-export protein MTP1 in lung cells. *Am J Physiol Lung Cell Mol Physiol* 283: L932–L939, 2002.
27. **Yeh KY, Yeh M, Glass J.** Hepcidin regulation of ferroportin 1 expression in the liver and intestine of the rat. *Am J Physiol Gastrointest Liver Physiol* 286: G385–G394, 2004.